

Subcellular Localization of Thiol-Capped CdTe Quantum Dots in Living Cells

Yu Zhang · Lan Mi · Rongling Xiong · Pei-Nan Wang ·
Ji-Yao Chen · Wuli Yang · Changchun Wang ·
Qian Peng

Received: 12 August 2008 / Accepted: 17 October 2008 / Published online: 5 April 2009
© to the authors 2009

Abstract Internalization and dynamic subcellular distribution of thiol-capped CdTe quantum dots (QDs) in living cells were studied by means of laser scanning confocal microscopy. These unfunctionalized QDs were well internalized into human hepatocellular carcinoma and rat basophilic leukemia cells *in vitro*. Co-localizations of QDs with lysosomes and Golgi complexes were observed, indicating that in addition to the well-known endosome-lysosome endocytosis pathway, the Golgi complex is also a main destination of the endocytosed QDs. The movement of the endocytosed QDs toward the Golgi complex in the perinuclear region of the cell was demonstrated.

Keywords Cells · Confocal microscopy · Imaging · Quantum dots · Subcellular localization

Electronic supplementary material The online version of this article (doi:10.1007/s11671-009-9307-9) contains supplementary material, which is available to authorized users.

Y. Zhang · L. Mi · R. Xiong · P.-N. Wang (✉)
Department of Optical Science and Engineering, Key Lab for Advanced Photonic Materials and Devices, Fudan University, Shanghai 200433, China
e-mail: pnwang@fudan.edu.cn

J.-Y. Chen (✉)
Surface Physics Laboratory (National Key Lab) and Department of Physics, Fudan University, Shanghai 200433, China
e-mail: jychen@fudan.edu.cn

W. Yang · C. Wang
Department of Macromolecular Science and Key Lab of Molecular Engineering of Polymers, Fudan University, Shanghai 200433, China

Q. Peng
Department of Pathology, The National Hospital-Norwegian Radium Hospital, University of Oslo, Montebello, Oslo, Norway

Introduction

Water-soluble colloidal semiconductor quantum dots (QDs) are a new class of fluorescent probes with excellent optical properties. Researches have recently been focused not only on their photoluminescence (PL) behaviors [1, 2], but also on their biomedical applications of labeling of cells, protein trafficking, DNA array technology, and immunofluorescence assays [3–7]. Fluorescence labeling and tracking of subcellular organelles and proteins are considered as a powerful tool to reveal the mystery of cellular activities. The sufficient brightness and photostability make QDs favorable for tracking intracellular events.

The first step for intracellular delivery of QDs is to cross the cell membrane barrier [8–14]. It is reported that surface functionalized QDs can effectively be internalized into cells and ended up in endosomes/lysosomes [8, 9, 15]. Ruan et al. [14] have shown that the Tat peptide-conjugated QDs were initially trapped in vesicles and then transported to the intracellular region corresponding to the microtubule organizing center. Although water-soluble QDs without surface bioconjugations were considered to be difficult to enter into cells [15], the internalizations of unfunctionalized QDs into living cells were reported [1, 2]. Recently, Nabiev et al. [16] observed that the unfunctionalized QDs with a small size of 2.1 nm were actively transported to the nucleus in macrophages, while QDs with a size of 3.8 nm did not enter the nucleus.

Endocytosis is believed as the main mechanism of intracellular delivery of QDs, but the endocytic process is complicated with several possible pathways. Moreover, the internalization process of a particle is a dynamic course with various destinations [17–19]. So far, little is known concerning the endocytic route of QDs in cells. The aim of this study was to examine subcellular localization patterns

of the thiol-capped CdTe QDs in living cells by means of confocal microscopy. This report shows that QDs are localized not only in lysosomes, but also in Golgi complexes of the human hepatocellular carcinoma (QGY) and rat basophilic leukemia (RBL) cell lines.

Experimental Details

The water-soluble thiol-capped CdTe QDs were prepared via the modified hydrothermal route using the thiolglycolic acid as a stabilizer [20]. Briefly, by a molar ratio of 2:1, sodium borohydride was used to react with tellurium in water to prepare the sodium hydrogen telluride (NaHTe). Fresh solutions of NaHTe were diluted with N₂-saturated deionized water to 0.0467 M for further use. CdCl₂ (1 mmol) and thioglycolic acid (1.2 mmol) were dissolved in 50 mL of deionized water. Stepwise addition of NaOH solution adjusted the precursors solution to pH = 9. Then, 0.096 mL of oxygen-free solution containing fresh NaHTe, cooled to 0 °C, was added into 10 mL of the above precursor solution and vigorously stirred. Finally, the solution with a faint yellow color was put into a Teflon-lined stainless steel autoclave with a volume of 15 mL. The autoclave was maintained at the reaction temperature (200 °C) for a certain time and then cooled to the room temperature by a hydro-cooling process.

The core diameter of the QDs used in this work was around 3.5 nm with an emission peak at 601 nm as shown in Fig. 1. The average hydrodynamic diameter of the QDs was around 28 nm as measured by the method of dynamic light scattering (Malvern, Autoszer 4700).

LysoTracker Green DND-26, BODIPY FL C₅-ceramide complexed to BSA and MitoFluor Green were used as indicators for lysosomes, Golgi complex and mitochondria,

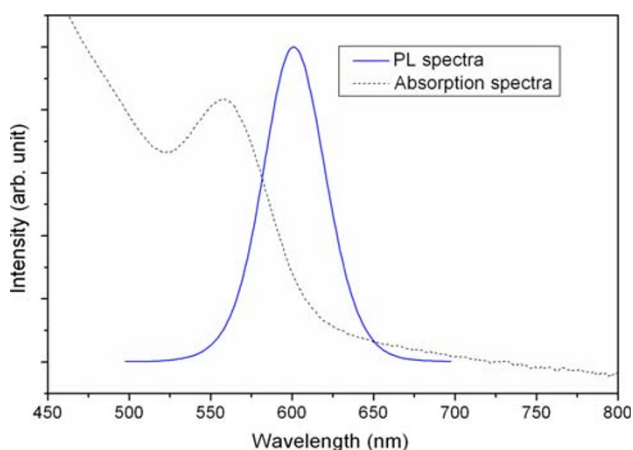


Fig. 1 Absorption and PL spectra of thiol-capped CdTe QDs in an aqueous solution

respectively. The emission peaks of these indicators are all around 511 nm.

The co-incubation of QGY (or RBL) cells with QDs and the fluorescent marker (LysoTracker, Golgi body marker, or MitoTracker) was carried out as follows: cells obtained from the Cell Bank of Shanghai Science Academy were seeded onto a glass cover slip placed in a culture dish containing DMEM-H medium with 10% fetal bovine serum, 100 $\mu\text{g mL}^{-1}$ streptomycin and 100 $\mu\text{g mL}^{-1}$ neomycin. The cells were then cultured in a fully humidified incubator at 37 °C with 5% CO₂ for their attachment to the cover slip. When the cells reached 80% confluence, the QD aqueous solution with a QD concentration of 50–100 $\mu\text{g mL}^{-1}$ plus the LysoTracker (100 nM), Golgi body marker (5 μM) or MitoTracker (100 nM) in the growth medium were added into the culture dish [9]. The cells were incubated for 30–60 min in an incubator before the subcellular localization pattern of the QDs was studied. The cells were kept at 37 °C during the microscopic examination using a temperature controller (Olympus).

The fluorescence images of the intracellular QDs and the markers for lysosome, Golgi complex and mitochondria were acquired with a laser scanning confocal microscope (Olympus, FV-300, IX71) using a 488 nm Ar⁺ laser (MELLES GRIOT) as the excitation source and a 60 \times oil objective to focus the laser beam. The fluorescence micrographs of QDs and the fluorescent marker (LysoTracker, Golgi body marker, or MitoTracker) were recorded simultaneously in two channels of the microscope with a 585–640 nm bandpass filter for QDs and a 505–550 nm bandpass filter for the fluorescent markers. Using the t-scan mode (30 s per frame with 2.8 s exposure time) of the microscope, the dynamic distributions of QDs, lysosomes, Golgi bodies and mitochondria were studied.

Results and Discussion

The time-dependent fluorescence images of lysosomes (green) and QDs (red) in RBL cells are depicted in Fig. 2. With an incubation time of 30 min, the cytoplasm membrane was stained with QDs and some QDs began to appear inside the cells. Further, the kinetic fluorescence images revealed that, from 30 min to 1 h, more QDs were transported into cells. From the merged image in Fig. 2c, it can be seen that many of the lysosomes only showed the green LysoTracker color at an early time (30 min), indicating there were no QDs in these lysosomes; while at a later time (55 min), most lysosomes showed a yellow color (a color representing the mixed fluorescence from LysoTracker and QDs), demonstrating the co-localization of QDs with these lysosomes occurred. Same circumstances were observed for QGY cells as well, in which more QDs were localized in

Fig. 2 Time-dependent fluorescence micrographs of the distributions of lysosomes and QDs in RBL cells. **a** The distribution of lysosomes (green), **b** the distribution of QDs (red), **c** the merged image of **(a)** and **(b)** in which the yellow color denotes the mixed fluorescence from QDs and LysoTracker, and **d** differential interference contrast (DIC) micrograph

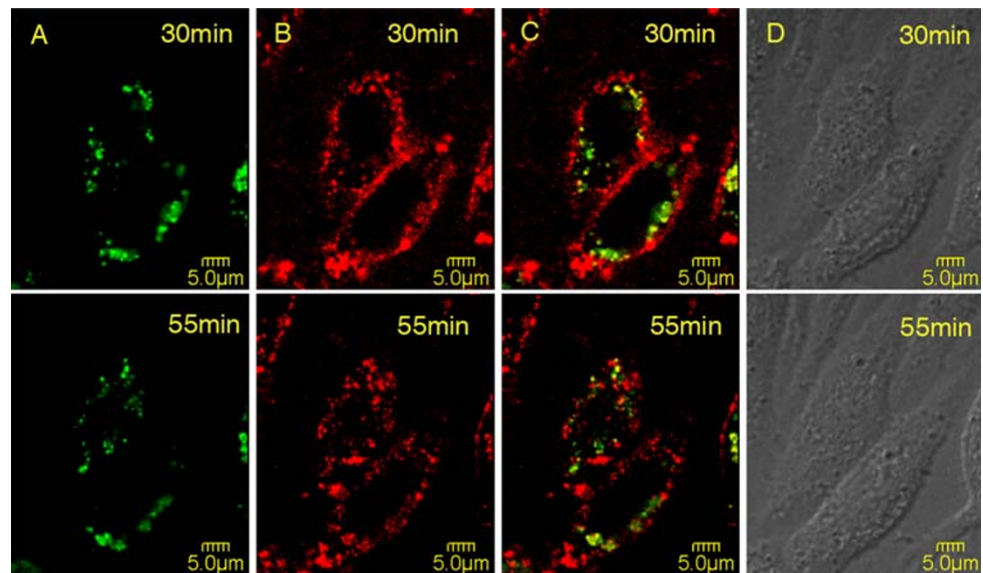
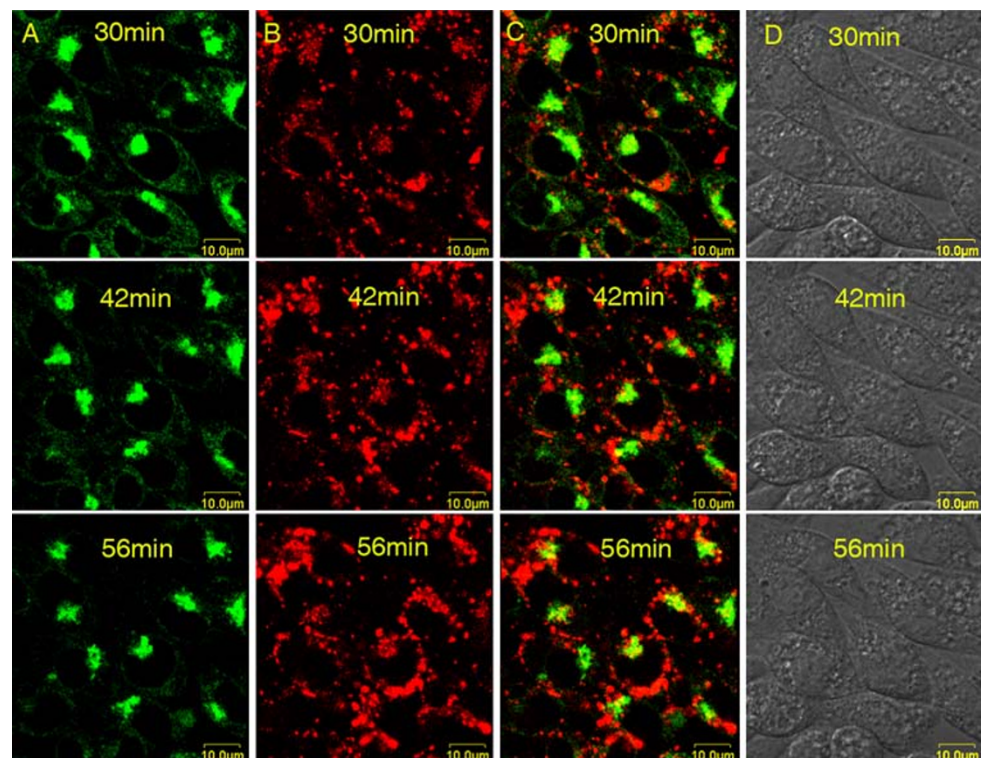


Fig. 3 Time-dependent fluorescence micrographs of the distributions of Golgi complexes and QDs in RBL cells. **a** The distribution of Golgi complexes (green), **b** the distribution of QDs (red), **c** the merged image of **(a)** and **(b)** in which the yellow color denotes the mixed fluorescence from QDs and Golgi marker, and **d** DIC micrograph



lysosome at a later time (see Supporting Information, Figure S1). Similar findings were reported by others, suggesting an endosome/lysosome pathway for the endocytosis of QDs [7, 9, 14, 15, 21].

However, Fig. 2c also reveals that there are still many QDs showing the red color, indicating that these QDs were localized in other sites than endosomes/lysosomes in the cell. On the basis of the previous reports [17, 18, 22] that

Golgi complex was also a principal intracellular destination of internalized molecules and particles, we employed BODIPY FL C5-ceramide complexed to BSA as the Golgi marker to examine if QDs could be localized in Golgi complex. The fluorescence micrographs to show the time-dependent distributions of Golgi complex and QDs in RBL and QGY cells are depicted in Figs. 3 and 4, respectively. It can be seen clearly that many of the endocytosed QDs

Fig. 4 Time-dependent fluorescence micrographs of the distributions of Golgi complexes and QDs in QGY cells. **a–d** Images as described in Fig. 3

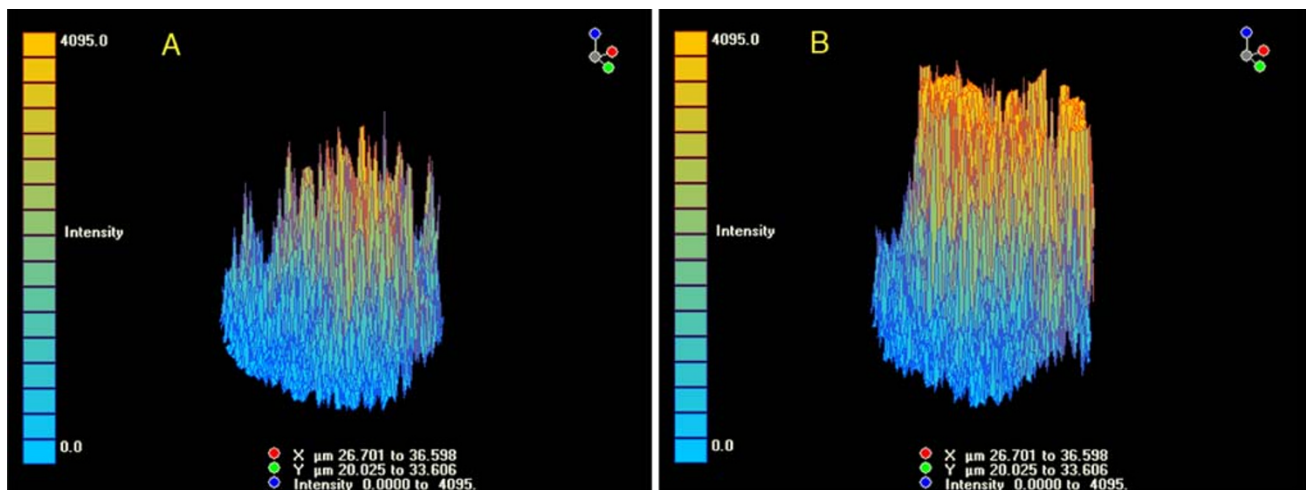
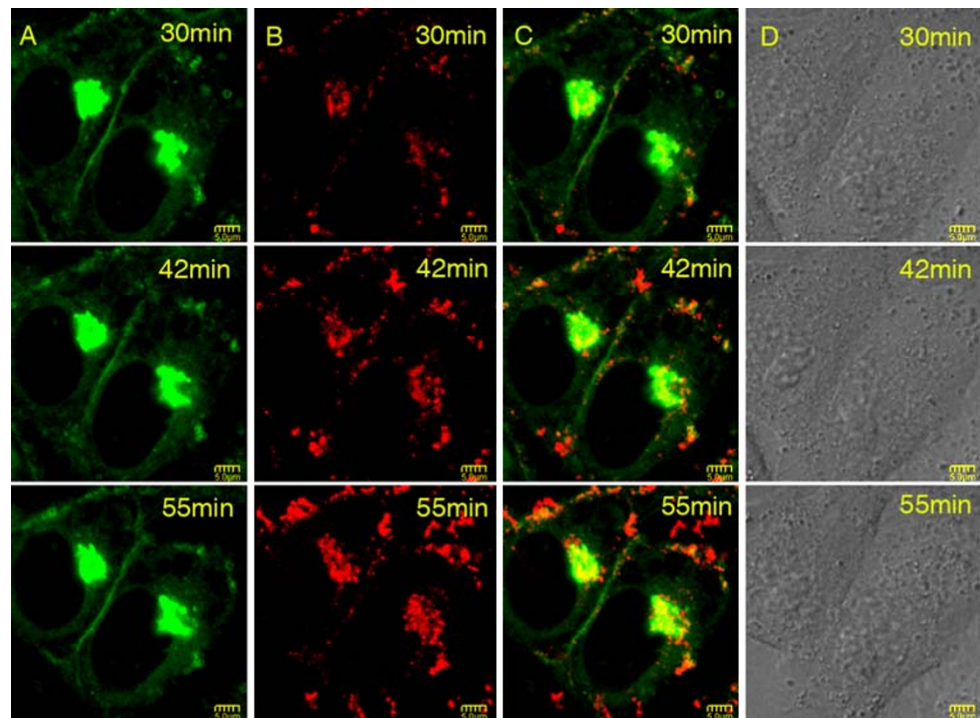


Fig. 5 Distribution of fluorescent intensity of QDs in an area co-localized with Golgi complex in a QGY cell: **a** 30 min and **b** 55 min

were gradually transported to the Golgi complexes in cells, indicating the co-localization of QDs with Golgi bodies. One hour later, almost all the Golgi complexes were filled with QDs, providing evidence that the Golgi complex is also an important terminal target of these thiol-capped CdTe QDs. In QGY cells, with an incubation time of 55 min, the distribution of QDs shows a similar shape as that of Golgi complexes (Fig. 4a, b). Then 55 min later, most of the Golgi complexes were filled with QDs, demonstrating that the Golgi complex is also an important terminal target of these thiol-capped CdTe QDs.

To obtain the quantitative data of the co-localization of QDs with Golgi complexes over time, we selected a Golgi complex area in a QGY cell in Fig. 4 to analyze the time-dependent fluorescence intensity of QDs using the software of Flouview supplied by Olympus. The results are shown in Figs. 5 and 6. It can be seen clearly in Fig. 5 that the fluorescence intensity was much stronger at a later time. Figure 6 shows that the fluorescence intensity increased almost linearly during the incubation period from 30 to 55 min, demonstrating a gradual increase of the amount of QDs transported into Golgi complexes.

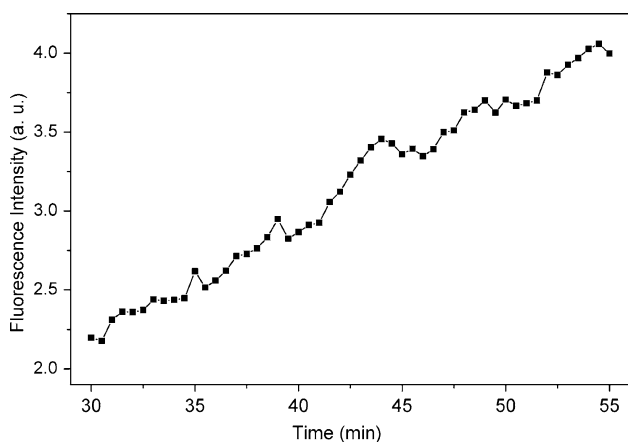


Fig. 6 Fluorescence intensity of QDs as a function of time in an area co-localized with Golgi complex in a QGY cell

Some enlarged micrographs to show a movement of endocytosed QDs (marked with arrow) toward the Golgi complex in the perinuclear region of a QGY cell are demonstrated in Fig. 7. This movement may be caused by a microtubule-dependent transport mechanism, an active process that is mediated by molecular motors such as dyneins [14].

The mitochondrial localization of QDs was also studied for RBL (Fig. 8) and QGY (see Figure S2 in Supporting Information) cells. After 1 h incubation of QDs, only a few

mitochondria were stained with QDs, indicating that the mitochondrion is not the main site of the QD distribution.

Conclusions

The understanding of the cellular delivery and subcellular distribution of QDs are of particular importance for cellular labeling with QDs, especially the labeling of subcellular compartments. Although QDs without surface bioconjugations were reported to be difficult to enter into cells [15], the thiol-capped CdTe QDs used in this work could be well internalized into living cells in vitro over a time period of about 1 h. This is probably due to the fact that the surface of the thiol-capped QD contains carboxylic groups, which may function as the biological interfacing [5]. There are complex and interconnected pathways that can carry molecules to various destinations within the endosomal system. It is well known that the cellular delivery of QDs is mediated through the endocytic route with the destinations of endosomes/lysosomes. The finding from this study shows that in addition to the endosome-lysosome endocytosis pathway, Golgi complex is also a main destination of the CdTe QDs, although the mechanism is not clear yet. This new finding not only provides information about the delivery of intracellular QDs, but will also be important toward the design and development of nanoparticle probes for intracellular imaging and therapeutic applications.

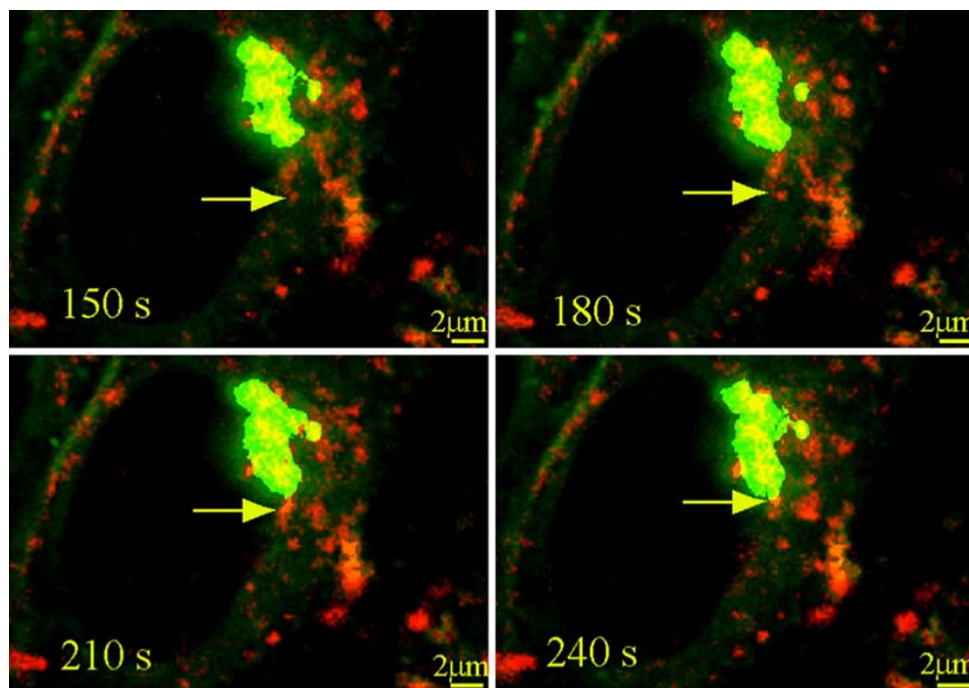


Fig. 7 Active transportation of the endocytosed QDs (arrow) toward a Golgi complex in a QGY cell

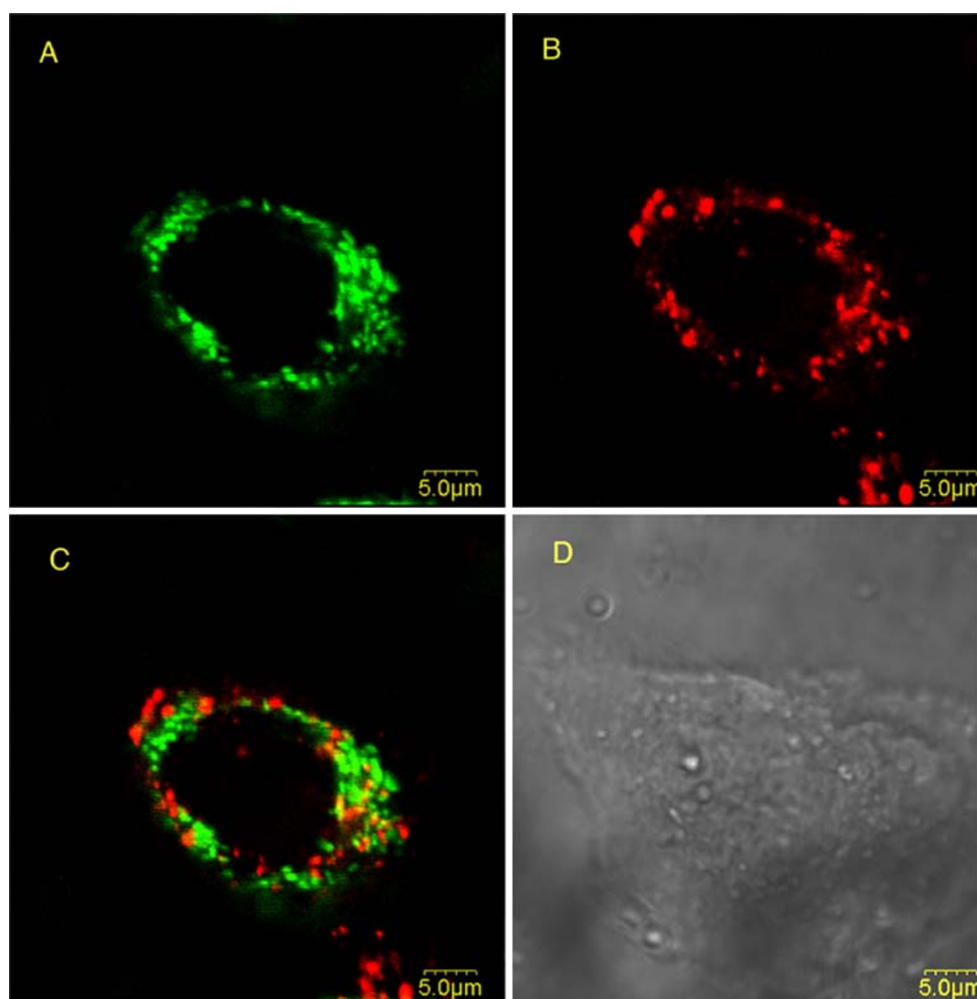


Fig. 8 Fluorescence micrographs of the distributions of mitochondria and QDs in RBL cells after 1 h incubation. **a** The distribution of mitochondria (green), **b** the distribution of QDs (red), **c** the merged

image of **(a)** and **(b)** in which the yellow color denotes the mixed fluorescence from QDs and MitoFluor, and **d** DIC micrograph

Acknowledgments This work was supported by National Natural Science Foundation of China (60638010, 10774027, 50525310), and Shanghai Municipal Science and Technology Commission (06ZR14005, 05QMX1404).

References

1. Y.H. Sun, Y.S. Liu, P.T. Vernier, C.H. Liang, S.Y. Chong, L. Marcu, M.A. Gundersen, *Nanotechnology* **17**, 4469 (2006). doi:[10.1088/0957-4484/17/17/031](https://doi.org/10.1088/0957-4484/17/17/031)
2. Y. Zhang, J. He, P.N. Wang, J.Y. Chen, Z.J. Lu, D.R. Lu, J. Guo, C.C. Wang, W.L. Yang, *J. Am. Chem. Soc.* **128**, 13396 (2006). doi:[10.1021/ja061225y](https://doi.org/10.1021/ja061225y)
3. P. Alivisatos, *Nat. Biotechnol.* **22**, 47 (2004). doi:[10.1038/nbt927](https://doi.org/10.1038/nbt927)
4. I.L. Medintz, H.T. Uyeda, E.R. Goldman, H. Mattouss, *Nat. Mater.* **4**, 435 (2005). doi:[10.1038/nmat1390](https://doi.org/10.1038/nmat1390)
5. X. Michalet, F.F. Pinaud, L.A. Bentolila, J.M. Tsay, S. Doose, J.J. Li, G. Sundaresan, A.M. Wu, S.S. Gambhir, S. Weiss, *Science* **307**, 538 (2005). doi:[10.1126/science.1104274](https://doi.org/10.1126/science.1104274)
6. W.J. Parak, T. Pellegrino, C. Plank, *Nanotechnology* **16**, R9 (2005). doi:[10.1088/0957-4484/16/2/R01](https://doi.org/10.1088/0957-4484/16/2/R01)
7. O. Seleverstov, O. Zabirnyk, M. Zscharnack, L. Bulavina, M. Nowicki, J.-M. Heinrich, M. Yezhelyev, F. Emmrich, R. O'Regan, A. Bader, *Nano Lett.* **6**, 2826 (2006). doi:[10.1021/nl0619711](https://doi.org/10.1021/nl0619711)
8. A. Cambi, D.S. Lidke, D.J. Arndt-Jovin, C.G. Figdor, T.M. Jovin, *Nano Lett.* **7**, 970 (2007). doi:[10.1021/nl0700503](https://doi.org/10.1021/nl0700503)
9. S.J. Cho, D. Maysinger, M. Jain, B. Röder, S. Hackbarth, F.M. Winnik, *Langmuir* **23**, 1974 (2007). doi:[10.1021/la060093j](https://doi.org/10.1021/la060093j)
10. S.B. Courty, C. Luccardini, Y. Bellaïche, G. Cappello, M. Dahan, *Nano Lett.* **6**, 1491 (2006). doi:[10.1021/nl060921t](https://doi.org/10.1021/nl060921t)
11. A.M. Derfus, W.C.W. Chan, S.N. Bhatia, *Adv. Mater.* **16**, 961 (2004). doi:[10.1002/adma.200306111](https://doi.org/10.1002/adma.200306111)
12. X.L. Nan, P.A. Sims, P. Chen, X.S. Xie, *J. Phys. Chem. B* **109**, 24220 (2005). doi:[10.1021/jp056360w](https://doi.org/10.1021/jp056360w)
13. S.S. Rajan, T.Q. Vu, *Nano Lett.* **6**, 2049 (2006). doi:[10.1021/nl0612650](https://doi.org/10.1021/nl0612650)
14. G. Ruan, A. Agrawa, A.I. Marcusan, S.M. Nie, *J. Am. Chem. Soc.* **129**, 14759 (2007). doi:[10.1021/ja074936k](https://doi.org/10.1021/ja074936k)
15. J. Silver, W. Ou, *Nano Lett.* **5**, 1445 (2005). doi:[10.1021/nl050808n](https://doi.org/10.1021/nl050808n)

16. I. Nabiev, S. Mitchell, A. Davies, Y. Williams, D. Kelleher, R. Moore, Y.K. Gun'ko, S. Byrne, Y.P. Rakovich, J.F. Donegan, A. Sukhanova, J. Conroy, D. Cottell, N. Gaponik, A. Rogach, Y. Volkov, *Nano Lett.* **7**, 3452 (2007). doi:[10.1021/nl0719832](https://doi.org/10.1021/nl0719832)
17. F.R. Maxfield, T.E. McGraw, *Nat. Rev. Mol. Cell Biol.* **5**, 121 (2004). doi:[10.1038/nrm1315](https://doi.org/10.1038/nrm1315)
18. S. Mukherjee, R.N. Ghosh, F.R. Maxfield, *Physiol. Rev.* **77**, 759 (1997)
19. B.J. Nichols, *Nat. Cell Biol.* **4**, 374 (2002)
20. J. Guo, W.L. Yang, C.C. Wang, *J. Phys. Chem. B* **109**, 17467 (2005). doi:[10.1021/jp044770z](https://doi.org/10.1021/jp044770z)
21. W.J. Parak, R. Boudreau, M.L. Gros, D. Gerion, D. Zanchet, C.M. Micheel, S.C. Williams, A.P. Alivisatos, C. Larabell, *Adv. Mater.* **14**, 882 (2002). doi:[10.1002/1521-4095\(20020618\)14:12<882::AID-ADMA882>3.0.CO;2-Y](https://doi.org/10.1002/1521-4095(20020618)14:12<882::AID-ADMA882>3.0.CO;2-Y)
22. P. Watson, A.T. Jones, D.J. Stephens, *Adv. Drug Deliv. Rev.* **57**, 43 (2005). doi:[10.1016/j.addr.2004.05.003](https://doi.org/10.1016/j.addr.2004.05.003)